

PromptGAR: Flexible Promptive Group Activity Recognition

Zhangyu Jin¹ Andrew Feng¹ Ankur Chemburkar¹ Celso M. De Melo²

¹ University of Southern California, Institute for Creative Technologies

² Army Research Laboratory

{zjin, feng, achemburkar}@ict.usc.edu, celso.m.demelo.civ@army.mil

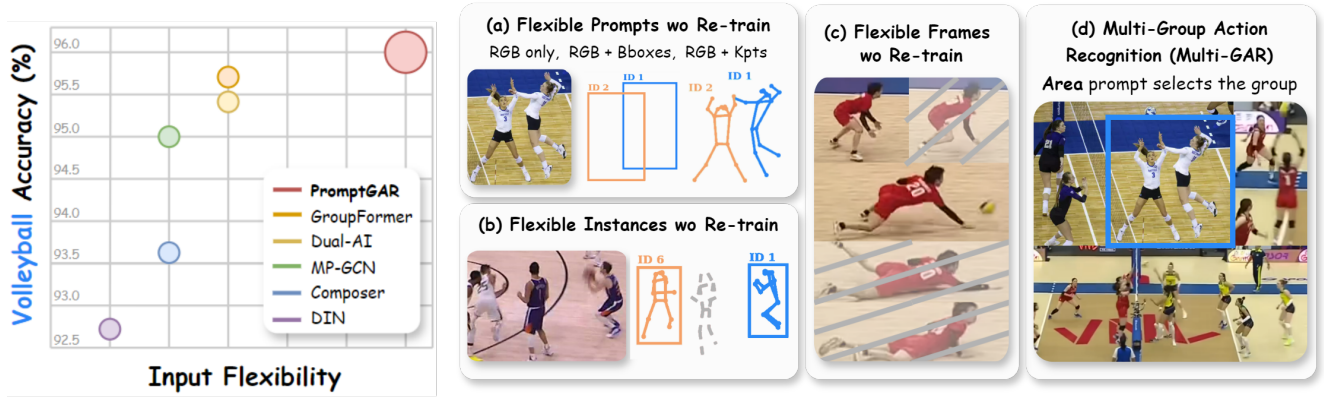


Figure 1. This diagram illustrates PromptGAR’s performance and key capabilities. Compared to existing methods, PromptGAR achieves competitive group activity recognition accuracy and superior input flexibility without the need for retraining, including: (a) flexible multi-modal prompt inputs, (b) flexible instance counts, and (c) flexible frame sampling. Additionally, (d) multi-group activity recognition is also supported by leveraging area prompts, enabling the selective recognition of the particular group activity within multiple groups.

Abstract

We present **PromptGAR**, a novel framework that addresses the limitations of current Group Activity Recognition (GAR) approaches by leveraging multi-modal prompts to achieve both input flexibility and high recognition accuracy. The existing approaches suffer from limited real-world applicability due to their reliance on full prompt annotations, the lack of long-term actor consistency, and under-exploration of multi-group scenarios. To bridge the gap, we proposed PromptGAR, which is the first GAR model to provide input flexibility across prompts, frames, and instances without the need for retraining. Specifically, we unify bounding boxes, skeletal keypoints, and areas as point prompts and employ a recognition decoder for cross-updating class and prompt tokens. To ensure long-term consistency for extended activity durations, we also introduce a relative instance attention mechanism that directly encodes instance IDs. Finally, PromptGAR explores the use of area prompts to enable the selective recognition of the particular group activity within videos that contain multiple concurrent groups. Comprehensive evaluations demon-

strate that PromptGAR achieves competitive performances both on full prompts and diverse prompt inputs, establishing its effectiveness on input flexibility and generalization ability for real-world applications.

1. Introduction

Group Activity Recognition (GAR) [8] is fundamentally important for video and event understanding, and it is widely used in areas such as video analytics, human computer interaction, and security systems. GAR processes videos and annotated information including bounding boxes, skeletons, ball trajectories, and optical flows to determine the group activity label. Building on prior research [55, 32, 15, 29, 19, 50, 36, 38], we aim to not only enhance group activity recognition accuracy but also to create a more flexible architecture capable of handling diverse prompt, frame, and instance inputs.

Although numerous models have been proposed, high-performance and flexible group activity recognition continues to be challenging due to the following difficulties:

Requirement for Full Prompts. Current high-

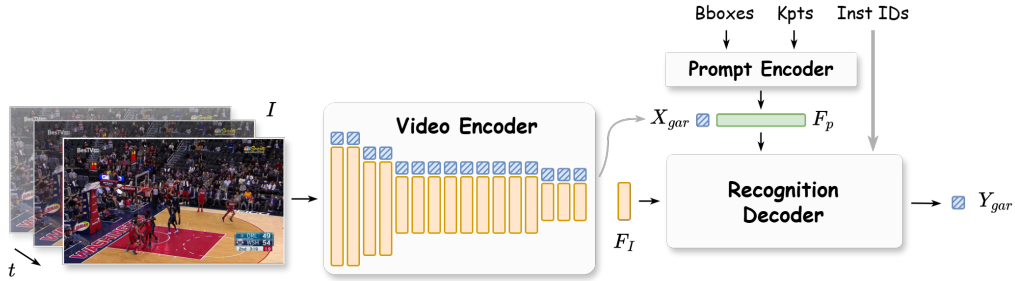


Figure 2. **PromptGAR Architecture.** A sequence of frames I is processed by the video encoder, yielding RGB features F_I and GAR class token X_{gar} . Prompts, such as bounding boxes and skeletal keypoints, are transformed to prompt tokens F_p by the prompt encoder. These tokens, along with instance IDs, are then fed into the recognition decoder for cross-modal updates to get group activity prediction Y_{gar} .

performance group activity recognizers [15, 29, 19] rely on full annotations to leverage all available modalities. This approach, however, makes their performance highly sensitive to the availability and quality of annotations. It is widely acknowledged that obtaining accurate human annotations is difficult. For instance, MP-GCN [32] uses automated tools like YOLOv8 [23] and BoTSORT [1] in NBA dataset [47] processing. However, the resulting annotations may include inaccuracies, such as false positives in background audiences, player ID switching, and ID reassignment upon reappearance. Despite utilizing state-of-the-art object detectors [56, 41], trackers [40, 49], and pose estimators [45, 16], the lower quality annotations such as inaccurate bounding boxes, missed detections, heavy occlusions, and redundant boxes from unreliable confidence scores may impact the resulting model accuracies and the real-world applicability for GAR.

Lacking Long-term Actor Consistency. Recent studies [55, 32, 15, 29, 19] prioritize short-term actor motions using optical flows or joint displacements between two neighboring frames. While effective for instantaneous activities like ‘spike’, ‘set’, and ‘pass’ in the Volleyball dataset, these methods struggle with longer activities. For instance, differentiating ‘3p-fail-offensive’ from ‘3p-succ’ and ‘3p-fail-defensive’ in the NBA dataset [47] requires recognizing a sequence of events: shooter location, ball trajectory, and subsequent ball possession. This highlights the critical importance of long-term consistency when activity duration and input frame length increase in real-world scenarios.

Under-explored Multi-Group Design. Current GAR methods [55, 32, 15, 29, 19] are limited to videos containing a single group, neglecting the common occurrence of multiple groups in real-world scenarios. This limitation, together with the difficulty of acquiring accurate annotations, calls for models capable of area-based prompts to easily select a particular group. Specifically, given a region of interest (ROI), the model should output the group activity label within that area. This becomes even more challenging when

groups move dynamically, with only the initial-frame ROI provided. Therefore, developing GAR models capable of accurately processing multi-group scenarios is crucial for bridging the gap between current research and real-world applicability.

Considering the above challenges and motivations, we present **PromptGAR**, a transformer-based group activity recognition framework that leverages multi-modal prompts (i.e., bounding boxes, skeletons, areas, or their combinations) to achieve high group activity recognition accuracy and input flexibility. (a) **Flexible Prompts.** It adapts to varying prompt availability, namely full prompts, partial prompts, and no prompts. When comprehensive annotations are present, the full prompt inputs would maximize performance. If only simpler annotations like bounding boxes and instance IDs are available, our model still gives reliable results. Even with no annotations, it can also provide reasonable results using only the raw video. This adaptability makes it suitable for diverse real-world scenarios where annotation quality varies. (b) **Flexible Frames.** The method has temporal flexibility in accepting videos of varying lengths and frame rates. Furthermore, it effectively recognizes group activities regardless of their temporal location within the video, accommodating both instantaneous actions and sequential events. (c) **Flexible Instances.** It is designed to handle varying numbers of actors within a scene. Therefore in an ideal scenario, our model can leverage detailed annotations of all individuals for enhanced accuracy. On the otherhand, it can also maintain robust performance even when there are missing annotations for certain actors. (d) **Without Retraining.** After training with full prompts, PromptGAR automatically gains the flexibility for input prompts, frames, and instances during inference. This significantly enhances its practicality and broadens its applicability to diverse scenarios.

Our implementation is inspired by the Segment Anything [25] by unifying bounding boxes, skeletons, and areas as point prompts and employing a two-way decoder for

cross-updating class and prompt tokens. **Firstly**, the input flexibility is implemented through several design features: MViTv2’s relative positional embedding for variable length of RGB frames, depth-wise prompt pooling to accommodate flexible temporal and modality dimensions, and a robust head that maintains classification stability even when no prompts are available during inference. **Secondly**, to effectively acquire long-term actor consistency, we introduce relative instance attention, which directly encodes instance IDs. The encoding ensures that the output will remain invariant to instance ID transitions. **Lastly**, PromptGAR introduces the use of area prompts, enabling the selective recognition of the particular group activity within videos that contain multiple concurrent groups.

Based on the above technical contributions, we evaluate our model under Volleyball [21] and NBA [47] datasets, PromptGAR produces competitive results compared to state-of-the-art GAR methods, showcasing its strong recognition capabilities. Additionally, we demonstrated its flexibility to handle varying prompt inputs, frame sampling, and instance counts while maintaining robust performance without retraining. To validate the ability to recognize specific groups within multi-group scenarios, we also performed experiment in multi-GAR with area prompts by synthetically creating a multi-group dataset. Our main contributions are as follows.

- (a) An effective group activity recognition architecture that achieves input flexibility across prompts, frames, and instances without retraining.
- (b) A relative instance attention module for encoding instance IDs and ensuring long-term actor consistency.
- (c) Demonstration of capability in multi-group activity recognition using area prompts.

2. Related Work

2.1. Group Activity Recognition

GAR [8] has attracted attention due to its massive success in a variety of real-world applications. Earlier techniques relied heavily on handcrafted features [8, 26, 18, 6, 9, 7, 34] or AND-OR graphs [2, 3, 39]. Recently, methods based on neural network architectures have been widely studied because of their ability to effectively extract features and fuse various modalities.

Various Modalities for GAR. (a) *RGB frames and bounding boxes.* Existing work either directly crops people from scenes [46] or applies ROIAlign [20] to represent actors from extracted feature maps [50, 38, 29]. (b) *Skeletons.* Several works [43, 55, 13, 32] explore using human skeleton joints as inputs to avoid substantial computational resources and discrepancies in background and camera settings in video-based approaches. (c) *Optical flows.* Neighboring RGB frames can produce optical flow images [52].

These flows are then concatenated with RGB frames to create dense inputs to introduce pixel-wise motion information across the temporal dimension [38, 29, 19]. A similar idea is also applied in Composer [55] for skeletal modality by computing the temporal difference of coordinates in two consecutive frames. MP-GCN [32] calculated joint motions and bone motions as extra sparse inputs. (d) *Balls.* Group labels in the NBA dataset [47], such as ‘*2p-succ*’ and ‘*3p-succ*’, are closely related to ball positions; therefore, Composer [55] and MP-GCN [32] treat balls as additional inputs. However, it is difficult to leverage these specific model designs for general scenarios such as non-sports activity recognition. (e) *Tracked instance IDs.* Recent approaches [50, 29] use optical flows to describe only short-term motions without explicitly encoding instance IDs to preserve long-term actor consistency. We introduce a relative instance ID encoding mechanism to handle this long-neglected modality.

Input Flexibility for GAR. Due to the model design choices, recent works [55, 32, 15, 29, 19] have less input flexibility in group activity recognition. (a) *Flexible prompts.* A common limitation among GAR methods [15, 29, 19] that process RGB frames and bounding boxes is their dependence on ROIAlign [20] for actor feature extraction, making them incompatible with scenarios lacking bounding box prompts. Likewise, GroupFormer’s fixed input channel setting [29], achieved through concatenating RGB and skeleton features, prevents its use when skeleton data is unavailable. (b) *Flexible frames.* DualAI [19] demonstrates some flexibility by applying different frame sampling strategies during training and testing, such as 3 frames for training and 9 or 20 frames for testing on the Volleyball [21] and NBA [47] datasets, respectively. However, these frame counts remain significantly lower than the total available frames (41 for Volleyball, 72 for NBA) in each clip. This restricted frame sampling flexibility limits its potential for achieving higher performance. (c) *Flexible instances.* Composer [55] relies on normalizing joint coordinates with statistics derived from the complete clip. However, missing instances significantly alter these statistics, shifting the mean and standard deviation far from their expected distribution. Notably, our PromptGAR maintains high performance across inputs with flexible prompts, frames, and instances without the needs for retraining.

2.2. Multi-Group Activity Recognition

Previous research [55, 32, 15, 29, 19] in GAR are limited by having only a single group throughout the entire video. In such a case, all of the modalities, including bounding boxes, skeletons, optical flows, and instance IDs, are only served as ‘*enhancers*’ to add more clue on determining the group activities. In real-world situations, we are particularly interested in how well recognition works when *multiple*

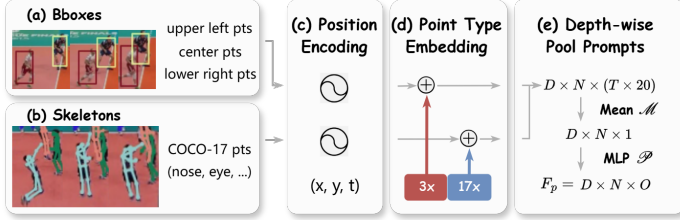


Figure 3. **Prompt Encoder.** (a) Bounding boxes are represented by 3 points (upper-left, center, lower-right). (b) Skeletal keypoints consist of 17 points. (c) Positional encoding captures both spatial and temporal coordinates. (d) Point types are distinguished using learnable embeddings. (e) Depth-wise prompts pooling reduces temporal and type dimensions to 1, then up-projects to the number of pooled prompts O .

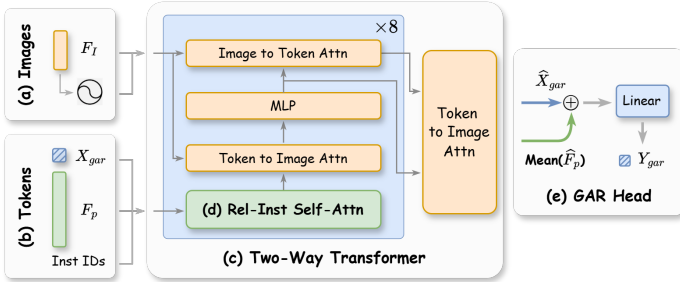


Figure 4. **Recognition Decoder.** The decoder processes (a) RGB features \mathbf{F}_I with positional embeddings and (b) the GEAR class token \mathbf{X}_{gar} and prompt tokens \mathbf{F}_p . (c) The Two-Way Transformer performs cross-updating between these features. (d) Relative instance self-attention, using instance IDs, ensures long-term actor consistency. (e) The GEAR head takes updated GEAR class token $\hat{\mathbf{X}}_{gar}$ and average of updated prompt tokens $\hat{\mathbf{F}}_p$ to predict the group activity label \mathbf{Y}_{gar} .

groups are present in the same video. Similar topics, such as spatio-temporal action detection [17, 28, 30], emphasize on accuracy of temporal intervals and spatial coordinate predictions to recognize individual actions rather than group ones. Therefore, we firstly introduce *multi-group activity recognition* (Multi-GAR), in which modalities act as both ‘*enhancers*’ and ‘*selectors*’ to choose the particular group activity in a video that contains multiple groups. Most GEAR methods [55, 32, 15, 29, 19] could be extended to Multi-GAR through bounding box or skeleton offsets. However, those methods are unable to process *area prompts*, a box defines the region of interest for a group activity. It acts only as a ‘*selector*’ for a group activity without requiring strong annotations for individual actors. In this paper, we explore multi-GAR problem with the proposed PromptGAR to effectively handles both regular modalities and *area prompts*.

3. Method

As shown in Fig. 2, PromptGAR is an end-to-end multi-modal prompt-based framework for group activity recognition. It takes a sequence of frames and corresponding prompts as inputs and outputs the group activity label. In the following subsection, we first introduce how to encode

videos and multi-modal prompts in §3.1. Then we illustrate how to fuse sparse-dense modalities and spatial-temporal information in §3.2. Finally, we introduce multi-group activity recognition and area prompts in §3.3.

3.1. Multi-Modality Inputs Encoding

PromptGAR supports three kinds of inputs: input frames \mathbf{I} , bounding box prompts \mathbf{F}_{box} , and skeleton prompts \mathbf{F}_{kpt} .

Video Encoding. While existing works [50, 19] have shown promises in their power to model RGB features, they focus on images rather than videos. Other studies [38, 29] chose I3D [5], but they require optical flows as extra dense guidance. To address those issues, the sequence of frames \mathbf{I} is processed through MViTv2 [31], to extract multi-scale feature tokens \mathbf{F}_I and the GEAR class token \mathbf{X}_{gar} .

Point Prompts. As shown in Fig. 3, all of the aforementioned prompts are formulated as point prompts: (a) Bounding boxes are formatted in three points, including upper-left, center, and lower-right points, similarly as in [25]. (b) Human skeletons follow the definition of COCO keypoints [33]. In general, one point is uniquely described by five attributes:

$$(x, y, t, p, ID)$$

where x, y, t are the positions along the width, height, and temporal axes, p is the point type, and ID denotes the instance identity that the point belongs to. We encode these attributes in the following ways. *Firstly*, while the original Fourier embedding [42] only maps the spatial coordinate (x, y) to the corresponding feature dimensions, we extend its capability to incorporate temporal location t .

$$\gamma(\mathbf{v}) = \left[\cos \left(2\pi \mathbf{B}(2\mathbf{v} - 1) \right), \sin \left(2\pi \mathbf{B}(2\mathbf{v} - 1) \right) \right]^T$$

where $\mathbf{v} := [x, y, t]^T \in [0, 1]^3$ is the spatial-temporal coordinate, and $\mathbf{B} \in \mathbb{R}^{\lfloor D/2 \rfloor \times 3}$ is sampled from a Gaussian distribution $\mathcal{N}(0, 1)$. The same positional encoding is also applied to RGB features \mathbf{F}_I . *Secondly*, we employ learned embeddings for each prompt type p , similar to [25]. *Thirdly*, ID is encoded by relative embeddings, with details in § 3.2.

Depth-wise Prompts Pooling. As described in Fig. 3-(e), after obtaining prompt features \mathbf{F}_{box} and \mathbf{F}_{kpt} , we employ a mean pooling operator \mathcal{M} and a MLP projector \mathcal{P} . They perform along temporal and type dimensions.

$$\mathbf{F}_p = (\mathcal{P} \circ \mathcal{M})([\mathbf{F}_{box}; \mathbf{F}_{kpt}])$$

where $\mathbf{F}_p \in \mathbb{R}^{D \times N \times O}$, $\mathbf{F}_{box} \in \mathbb{R}^{D \times N \times (T \times 3)}$ and $\mathbf{F}_{kpt} \in \mathbb{R}^{D \times N \times (T \times 17)}$. And D, N, T, O are the embedding size, number of instances, number of frames, and number of pooled prompts, respectively.

The pooling mechanism reduces the computational complexity and avoids out-of-memory (OOM) in the recognition decoder. The depth-wise mechanism, namely the

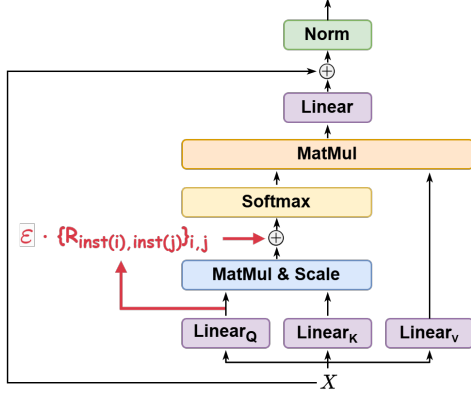


Figure 5. The **Relative Instance Attention** mechanism that incorporating a constant scale ϵ and relative instance embeddings $\mathcal{R}_{\text{inst}(i), \text{inst}(j)}$ in the attention block.

mean operator \mathcal{M} that reduces channels from $T \times 20$ to 1, is specifically designed for input flexibility across temporal and modality dimensions. Consequently, a model trained on T_1 frames can perform inference on T_2 frames ($T_2 \neq T_1$) without requiring architectural modifications or weight changes. Similarly, the model is able to infer with either bounding box prompts alone or skeleton prompts alone, even when trained on both modalities. Note that the instance dimension N is not pooled and is required by ID encoding in §3.2.

3.2. Cross-Modality Decoding

Leveraging the image embedding \mathbf{F}_I , the prompt features \mathbf{F}_p and associated instance IDs, PromptGAR takes the GAR class token \mathbf{X}_{gar} to decode the GAR logits \mathbf{Y}_{gar} .

Two-Way Transformer. For simplicity, we refer to these embeddings (not including the image embedding) collectively as "tokens".

$$\begin{aligned} \text{images} &= \mathbf{F}_I, \quad \text{tokens} = [\mathbf{X}_{gar}; \mathbf{F}_p] \\ \widehat{\mathbf{F}}_I, [\widehat{\mathbf{X}}_{gar}; \widehat{\mathbf{F}}_p] &= \text{Two-Way}(\text{images}, \text{tokens}) \end{aligned}$$

Our two-way transformer is shown in Fig. 4-(c), inspired by [25], each layer performs 4 steps: (1) relative instance self-attention on tokens, (2) cross-attention from tokens to the image embedding, (3) an MLP updates each token, and (4) cross-attention from the image embedding to tokens. The next layer takes the updated tokens and the updated image embedding from the previous layer. Input flexibility is well-achieved through the attention mechanism, which naturally handles inputs of different lengths. This allows our two-way transformer to process varying numbers of frames, types, or instances at inference time, regardless of those in training.

Relative Instance Attention. Existing research has demonstrated potential in modeling short-term temporal

consistency via either optical flows [38, 29, 19] or joint motions [55, 32]. As these methods primarily focus on capturing motion between immediate time steps, the long-term consistency in the movement of objects or individuals is not well handled. Also, the use of absolute instance ID encodings to ensure consistency violates the principle of shift invariance [27]. Namely, the interaction between two prompts becomes dependent on their arbitrary instance IDs , even if they refer to the same underlying object or entity. Inspired by relative positional embedding, we introduce the relative instance ID embedding to address this issue by focusing on whether two tokens belong to the same instance or not.

As illustrated in Fig. 5, we encode the relative instance information between the two input elements, i and j , into embedding $\{R_{\text{inst}(i), \text{inst}(j)}\}_{i,j} \in \mathbb{R}^D$, where $\text{inst}(i)$ and $\text{inst}(j)$ denote the instance ID of element i and j . Notice that the GAR class token \mathbf{X}_{gar} is not included in $E^{(rel)}$.

$$\text{Attn}(Q, K, V) = \text{Softmax}\left(\frac{QK^T}{\sqrt{d}} + \epsilon \cdot E^{(rel)}\right)V,$$

$$\text{where } E_{i,j}^{(rel)} = Q_i \cdot \{R_{\text{inst}(i), \text{inst}(j)}\}_{i,j}$$

Here, the number of token pairs belonging to different instances significantly outnumbers those belonging to the same instance. To address the imbalance problem, we assign a learnable embedding R to pairs of tokens within the same instance, while setting the embedding to 0 for pairs from different instances.

$$\{R_{\text{inst}(i), \text{inst}(j)}\}_{i,j} = \begin{cases} 0, & \text{inst}(i) \neq \text{inst}(j) \\ R, & \text{inst}(i) = \text{inst}(j) \end{cases}$$

Due to the sparsity of $E^{(rel)}$, the scaling factor ϵ is a constant determined by experiments, with details in §4.5. Note that relative instance embeddings cannot be applied to cross-attention between image embeddings and tokens, as image embeddings lack associated instance ID information.

GAR Head. In contrast to most approaches [12, 25, 31, 48], where [class] tokens are directly fed to MLP layers for logits prediction, we observe a unique challenge in GAR. While traditional methods align different prompts with distinct ground truth labels [25], in GAR, various prompts correspond to the same ground truth label. As illustrated in Fig. 4-(e), to encourage the network to utilize the information provided by the prompts, we add the class tokens with the averaged prompt features. Then a linear projection is employed to generate final logits for prediction.

$$\mathbf{Y}_{gar} = \text{Linear}\left(\widehat{\mathbf{X}}_{gar} + \text{Mean}(\widehat{\mathbf{F}}_p)\right)$$

where $\text{Mean}(\widehat{\mathbf{F}}_p) \in \mathbb{R}^D$ means taking average over $T \times O$.

Our approach is also carefully designed to ensure input flexibility, even when the prompts present during the training time are absent during the inference time. During back-



Figure 6. Left is the **2-Mosaic Volleyball Dataset**, showing two vertically concatenated clips. Right is the **4-Mosaic Volleyball Dataset** in the 2×2 format. In both cases, a target clip is randomly chosen from each position, and only the annotations corresponding to that target clip are present.

propagation, the gradients of $\widehat{\mathbf{X}}_{gar}$ and $\text{Mean}(\widehat{\mathbf{F}}_p)$ are identical, indicating they are optimized in the same direction and towards the same representation. Consequently, a well-trained model can function effectively using either $\widehat{\mathbf{X}}_{gar}$ or $\text{Mean}(\widehat{\mathbf{F}}_p)$ independently.

3.3. Multi-Group Activity Recognition

We extend the PromptGAR architecture for multi-group activity recognition. Specifically, an *area prompt* is defined to indicate the region of interest for a particular group activity within a video containing multiple groups. Similar to bounding boxes, it is formulated by three points: the upper-left, center, and lower-right. The prompt encoder then outputs \mathbf{F}_a , a tensor of shape $D \times 1 \times O$. The dimension $N = 1$ shows that only one area instance is being processed. The recognition decoder, following the same procedure, processes image embeddings \mathbf{F}_I and concatenated tokens $[\mathbf{X}_{gar}; \mathbf{F}_a]$ to generate the prediction \mathbf{Y}_{gar} . With the spatial awareness provided by ‘Area prompts’, our PromptGAR accurately identifies the target group activity.

4. Experiments

4.1. Experimental Setup

Volleyball Dataset [21] contains 3,493 clips for training and 1,337 clips for testing. Each clip has 41 frames and is labeled with one of eight group activities. Bounding box and skeleton annotations, provided separately by [21, 55], are available only for the central 16 frames of each clip. In approximately 20.5% of clips, bounding boxes are shifted substantially from their correct positions. Therefore we use skeleton-derived envelope bounding boxes instead. Skeleton annotations are also occasionally unreliable due to heavy occlusions or truncations in frame boundaries. Consistent with prior works, we limit our analysis for central 16 frames to avoid potential interference from additional group activities present in the remaining half of the clips.

NBA Dataset [47] includes 7,624 training clips and 1,548 testing clips. Each clip includes 72 frames and is categorized into nine group activity labels. Due to its increasing complexity, the NBA dataset demands special design and

Method	Modalities						Top1 Acc	Mean Acc
	RGB	Bbox	Kpt	Flow	Ball	InstID		
ARG [44]	✓	✓					90.7	91.0
HiGCIN [46]	✓	✓					91.4	92.0
DIN [50]	✓	✓					92.7*	92.8*
POGARS [43]			✓		✓		93.9	-
Composer [55]			✓		✓		93.6*	-
SkeleTR [13]			✓				94.4	-
MP-GCN [32]			✓		✓		95.0 [†]	95.0 [†]
CRM [4]	✓	✓		✓			93.0	-
ActorFormer [15]		✓	✓	✓			94.4	-
GIRN [37]	✓	✓	✓	✓			94.0	-
SACRF [38]	✓	✓	✓	✓			95.0	-
GroupFormer [29]	✓	✓	✓	✓			95.7	-
Dual-AI [19]	✓	✓		✓			95.4	-
KRGFormer [36]	✓	✓	✓				94.6	94.8
PromptGAR	✓	✓	✓			✓	96.0	96.3

Table 1. **Quantitative Comparisons in Volleyball Dataset.** (–) denotes not reported in the paper, (*) reproduced from released codes, (†) reproduced with keypoint-ball results (late-fusion parts un-released), and unmarked other methods are not open-sourced.

Method	Modalities						Top1 Acc	Mean Acc
	RGB	Bbox	Kpt	Flow	Ball	InstID		
ARG [44]	✓	✓					59.0	56.8
ActorFormer [15]	✓	✓		✓			47.1	41.5
SAM [47]	✓	✓					49.1	47.5
DIN [50]	✓	✓					61.6	56.0
Dual-AI [19]	✓	✓		✓			58.1	50.2
KRGFormer [36]	✓	✓					72.4	67.1
DFWSGAR [24]	✓						75.8	71.2
Flaming-Net [35]	✓			✓			79.1	76.0
MP-GCN [32]			✓		✓		75.8 [†]	72.0 [†]
PromptGAR	✓	✓	✓			✓	80.6	76.9

Table 2. **Quantitative Comparisons in NBA Dataset.** (†) reproduced with keypoint-ball results (late-fusion and multi-ensemble parts un-released), and unmarked methods are not open-sourced.

Method	Modalities					Re-train	2-Mosaic		4-Mosaic	
	RGB	Bbox	Kpt	InstID	Area		Top1	Mean	Top1	Mean
	✓	✓	✓	✓		✓	93.7	94.1	89.9	89.3
PromptGAR	✓				✓	✓	89.6	90.2	81.5	82.7
	✓					✓	54.0	53.6	23.5	23.0

Table 3. **Multi-Group Activity Recognition.** Area prompts provide reliable results, empowering PromptGAR to selectively recognize group activities in multi-group settings. Experiments are conducted under smaller models with $O = 16$.

processing compared to the Volleyball dataset [21]. Unlike Volleyball [21], we use all 72 frames in NBA because key event frames are not centrally located. Also, NBA activities are much longer than Volleyball’s. For example, ‘3p-fail-

offensive’ requires recognizing shooter location, ball trajectory, and possession.

Mosaic Volleyball Dataset. We generated a multi-group activity recognition dataset from the Volleyball dataset, as existing datasets [21, 47] are limited to single-group scenarios. As depicted in Fig. 6, we created two types of multi-group videos: *2-Mosaic* (two clips stacked vertically) and *4-Mosaic* (four clips arranged in a 2×2 grid). For each mosaic, the target clip is randomly assigned a position, and the remaining clips are uniformly selected from the Volleyball dataset. Annotations are derived from the target clip: its activity label is used for the entire mosaic, and its bounding boxes and skeleton data are adjusted based on its position. Area prompts are generated by creating a bounding envelope around all bounding boxes within each frame. We evaluate performance using Top-1 and Mean Accuracy.

Implementation details. We utilize the MViTv2-Base [31] video encoder with a 224×224 input resolution. For the Volleyball dataset [21], training and testing use the center 16 frames. The NBA dataset [47] is trained on 56 uniformly sampled frames and tested on all 72. The recognition decoder consists of an eight-layer stack of two-way transformers. All models are trained on 4 A100-80GB GPUs, where the Volleyball dataset use a batch size of 64, and the NBA dataset employ 24. Training runs for 200 epochs, using an AdamW optimizer and a Cosine Annealing learning rate scheduler. The initial learning rates are 2×10^{-4} for Volleyball and 7.5×10^{-5} for NBA.

4.2. Group Activity Recognition

Volleyball Dataset. In Tab. 1, we compare our method to the group activity recognition methods that rely on: (a) RGB frames, like DIN [50], which suffers from limited performance; (b) skeletons and ball trajectories, like Composer [55] and MP-GCN [32], which requires ball trajectories as extra inputs; (c) multi-modal techniques, like GroupFormer [29] and Dual-AI [19], which takes computationally expensive optical flows as inputs and thus sensitive to input frame rates. In contrast, our PromptGAR, without the drawbacks of those other modality inputs, still produces 96.0% top1 accuracy and 96.3% mean accuracy, achieving significant improvements across different baseline models.

NBA Dataset. Tab. 2 shows that PromptGAR significantly outperforms previous methods on the challenging NBA dataset [47]. This success is attributed to the instance ID modality, which provides stable long-term actor consistency, crucial for recognizing complex, multi-event group activities in longer videos.

4.3. Multi-Group Activity Recognition

As demonstrated in Tab. 3, even when provided with only the most basic *‘area prompts’* as minimal *‘selectors’* without any additional annotations, PromptGAR still

Method	Modalities				Re-train	Top1 Mean	
	RGB	Bbox	Kpt	Flow		InstID	Acc
GroupFormer [29]	✓	✓	✓	✓		95.7	-
	✓	✓		✓	✓	94.9	-
	✓	✓				94.1	-
PromptGAR	✓	✓	✓	✓		96.0	96.3
	✓		✓	✓	×	95.7	95.8
	✓	✓		✓		94.1	94.3
	✓					93.9	94.4

Table 4. **Flexible Prompts.** In the Volleyball dataset, we achieve remarkable performance under diverse prompts without retraining.

Method	Train		Test		Re-train	Top1 Mean	
	T	Sampling	T	Sampling		Acc	Acc
MP-GCN [32]	18	stride 1	18	stride 1	✓	73.3	68.4
	72	stride 1	72	stride 1		75.8	72.0
PromptGAR	56	uniform	36	stride 2	×	75.4	71.9
			56	stride 1		75.0	71.0
			64	stride 1		78.4	74.1
			72	stride 1		80.6	76.9

Table 5. **Flexible Frames.** For the NBA dataset, frames are all sampled at the center of each video clip. PromptGAR’s validation process also uses $T = 72$ to select the optimal checkpoint.

Method	# Instances	Re-train	Top1	Acc	Mean	Acc
PromptGAR	12	×	96.0	96.3		
	10		95.4	95.6		
	5		94.5	94.8		
	3		94.3	94.6		

Table 6. **Flexible Instances.** In the Volleyball dataset, instances are randomly deleted, and results are averaged over three trials.

achieved impressive recognition accuracy on multi-group mosaic videos. Specifically, it reaches top1 accuracy of 89.6% on the 2-Mosaic Volleyball dataset and 81.5% on the more complex 4-Mosaic Volleyball dataset. This demonstrates PromptGAR’s capability to effectively discern and recognize the particular group activity within multiple groups given the simple *‘area prompts’*.

4.4. Input Flexibility

Flexible Prompts. Tab. 4 demonstrates PromptGAR’s resilience to reduced prompt information. Using only skeleton data, it loses a negligible 0.3% in accuracy. When relying solely on bounding boxes, it achieves the same accuracy as GroupFormer [29], but without retraining. Even with only RGB input, the model’s accuracy remains reasonable, only 2.1% lower than with full prompts. This shows PromptGAR’s robustness to maintain high performance even with significantly reduced prompt inputs without retraining.

Flexible Frames. Tab. 5 exhibits PromptGAR’s adaptability to various frame sampling configurations. Although trained on 56 frames with the NBA dataset, it can effectively handle both shorter and longer sequences at test time. Specifically, it achieves 75.4% accuracy when tested with 36 frames (stride 2), nearly matching MP-GCN’s performance, which needs to be trained and tested on the full 72 frames specifically. Moreover, PromptGAR also outperforms MP-GCN when tested on all 72 frames, even though MP-GCN is optimized for this exact frame count. Furthermore, the effective rollout length during testing is crucial. When testing with 56 frames and a stride of 1, we see a 0.4% accuracy decrease compared to 36 frames with a stride of 2, due to the shorter rollout length (56 vs. 72). Those results demonstrate PromptGAR’s robust ability to handle diverse frame inputs without the need for retraining, a clear advantage over methods requiring retraining.

Flexible Instances. Tab. 6 showcases that PromptGAR can maintain high performance even when tested with fewer instances than it was trained on, without requiring retraining. To ensure a fair comparison, instances were randomly selected, and results were averaged over three experiments. Reducing from 12 instances to 10 results in only a 0.6% accuracy drop, and even when reduced to just 3 instances, the drop is still manageable at 1.7%. This highlights PromptGAR’s ability to function with reduced input, without the needs for retraining.

4.5. Ablation Studies

Tab. 7 details the impact of our novel modules on performance, starting with a baseline of 96.0% top-1 accuracy on the Volleyball dataset. (a) **Relative instance attention.** Eliminating instance IDs during training and testing resulted in a 0.6% drop in top-1 accuracy. This confirms that instance IDs are vital for encoding long-term consistency, enhancing performance. Furthermore, relative instance attention also accelerated training convergence. (b) **Prompt tokens in head.** Removing prompt tokens $\hat{\mathbf{F}}_p$ from the head, leaving only the GAR class token $\hat{\mathbf{X}}_{gar}$, led to a 0.3% accuracy decrease. This highlights the necessity of explicitly incorporating prompt tokens. Without them, the model struggles to integrate multi-modal prompt features, as the GAR class token alone sufficiently captures RGB information. (c) **No prompts.** Disabling the entire prompt encoder, using only the GAR class token $\hat{\mathbf{X}}_{gar}$ as input for the recognition decoder and the head, further reduced accuracy by 0.8%. This underscores the contribution of multi-modal prompt inputs in PromptGAR. Crucially, even without any prompts during training and testing, our model still compares favorably with other prompt-based baseline methods. Specifically, it achieves a 1.6% higher accuracy than DIN, which utilizes both RGB frames and bounding boxes, and a 0.7% higher accuracy than Composer, which uses skeletons

Method	Re-train	Top1 Acc	Mean Acc
PromptGAR	✓	95.8	96.0
<i>wo inst IDs</i>	✓	95.4	95.6
<i>wo prompt tokens in head</i>	✓	95.1	95.4
<i>no prompts</i>	✓	94.3	94.7

Table 7. **Effectiveness of Novel Modules.** Experiments are conducted using smaller models with $O = 16$ in Volleyball. Ablation studies included: ‘*wo inst IDs*’, where relative instance attention is replaced with regular self-attention; ‘*wo prompt tokens in head*’, where only the GAR class token \mathbf{X}_{gar} is used for the GAR head; and ‘*no prompts*’, where the recognition decoder receives only the GAR class token \mathbf{X}_{gar} and RGB features \mathbf{F}_I as inputs.

and ball trajectories as additional information. This demonstrates the superior ability of our MViTv2 architecture to process spatial-temporal information within only the RGB features compared to other backbones that process the video frame-by-frame separately.

5. Limitations and Future Works

Despite its competitive GAR accuracy and input flexibility, PromptGAR faces limitations with input resolution. (a) The input resolution is restricted to 224×224 , which is significantly lower than 1080×720 in other methods [50, 29, 19], due to MViTv2’s 3D convolutions and corresponding CUDA memory limitations. (b) In order to prevent out-of-memory *OOM* errors, only the smallest one from the MViTv2’s multi-scale feature maps ($8 \times 7 \times 7$ in the Volleyball dataset) can be utilized.

For future works, our research will explore several avenues to further enhance and validate PromptGAR’s capabilities. Firstly, given its support for single-actor prompts, we aim to assess its generalization capabilities on challenging action recognition tasks. Furthermore, to extend the experiments on multi-group GAR beyond the synthetic video mosaic dataset, we plan to evaluate PromptGAR on more complex datasets like MEVA [10], which features larger spatial movement, smaller actors, and human-vehicle group activities.

6. Conclusion

In this work, we present PromptGAR, a novel framework that addresses the limitations of current Group Activity Recognition (GAR) approaches by leveraging multi-modal prompts to achieve both input flexibility and high recognition accuracy. Extensive experiments show that PromptGAR allows the input flexibility across prompts, frames, and instances without the need for retraining. Furthermore, we introduce a novel relative instance attention mechanism that directly encodes instance IDs, ensuring long-term consistency for extended activity durations. Finally, Prompt-

GAR also uses the area prompts to enable the selective recognition of the particular group activity among multiple concurrent groups. Extensive evaluation validates the effectiveness and generalizability of our model.

References

- [1] N. Aharon, R. Orfaig, and B.-Z. Bobrovsky. Bot-sort: Robust associations multi-pedestrian tracking. *arXiv preprint arXiv:2206.14651*, 2022.
- [2] M. R. Amer, S. Todorovic, A. Fern, and S.-C. Zhu. Monte carlo tree search for scheduling activity recognition. In *Proceedings of the IEEE international conference on computer vision*, pages 1353–1360, 2013.
- [3] M. R. Amer, D. Xie, M. Zhao, S. Todorovic, and S.-C. Zhu. Cost-sensitive top-down/bottom-up inference for multiscale activity recognition. In *Computer Vision—ECCV 2012: 12th European Conference on Computer Vision, Florence, Italy, October 7–13, 2012, Proceedings, Part IV 12*, pages 187–200. Springer, 2012.
- [4] S. M. Azar, M. G. Atigh, A. Nickabadi, and A. Alahi. Convolutional relational machine for group activity recognition. In *Proceedings of the IEEE/CVF Conference on Computer Vision and Pattern Recognition*, pages 7892–7901, 2019.
- [5] J. Carreira and A. Zisserman. Quo vadis, action recognition? a new model and the kinetics dataset. In *proceedings of the IEEE Conference on Computer Vision and Pattern Recognition*, pages 6299–6308, 2017.
- [6] Z. Cheng, L. Qin, Q. Huang, S. Jiang, and Q. Tian. Group activity recognition by gaussian processes estimation. In *2010 20th International Conference on Pattern Recognition*, pages 3228–3231. IEEE, 2010.
- [7] W. Choi and S. Savarese. A unified framework for multi-target tracking and collective activity recognition. In *Computer Vision—ECCV 2012: 12th European Conference on Computer Vision, Florence, Italy, October 7–13, 2012, Proceedings, Part IV 12*, pages 215–230. Springer, 2012.
- [8] W. Choi, K. Shahid, and S. Savarese. What are they doing?: Collective activity classification using spatio-temporal relationship among people. In *2009 IEEE 12th international conference on computer vision workshops, ICCV Workshops*, pages 1282–1289. IEEE, 2009.
- [9] W. Choi, K. Shahid, and S. Savarese. Learning context for collective activity recognition. In *CVPR 2011*, pages 3273–3280. IEEE, 2011.
- [10] K. Corona, K. Osterdahl, R. Collins, and A. Hoogs. Meva: A large-scale multiview, multimodal video dataset for activity detection. In *Proceedings of the IEEE/CVF winter conference on applications of computer vision*, pages 1060–1068, 2021.
- [11] E. D. Cubuk, B. Zoph, J. Shlens, and Q. V. Le. Randaugment: Practical automated data augmentation with a reduced search space. In *Proceedings of the IEEE/CVF conference on computer vision and pattern recognition workshops*, pages 702–703, 2020.
- [12] A. Dosovitskiy. An image is worth 16x16 words: Transformers for image recognition at scale. *arXiv preprint arXiv:2010.11929*, 2020.
- [13] H. Duan, M. Xu, B. Shuai, D. Modolo, Z. Tu, J. Tighe, and A. Bergamo. Skeletr: Towards skeleton-based action recognition in the wild. In *Proceedings of the IEEE/CVF International Conference on Computer Vision*, pages 13634–13644, 2023.
- [14] R. Gao, Y. Zhang, and L. Wang. Multiple object tracking as id prediction. *arXiv preprint arXiv:2403.16848*, 2024.
- [15] K. Gavriluk, R. Sanford, M. Javan, and C. G. Snoek. Actor-transformers for group activity recognition. In *Proceedings of the IEEE/CVF conference on computer vision and pattern recognition*, pages 839–848, 2020.
- [16] Z. Geng, C. Wang, Y. Wei, Z. Liu, H. Li, and H. Hu. Human pose as compositional tokens. In *Proceedings of the IEEE/CVF Conference on Computer Vision and Pattern Recognition*, pages 660–671, 2023.
- [17] C. Gu, C. Sun, D. A. Ross, C. Vondrick, C. Pantofaru, Y. Li, S. Vijayanarasimhan, G. Toderici, S. Ricco, R. Sukthankar, et al. Ava: A video dataset of spatio-temporally localized atomic visual actions. In *Proceedings of the IEEE Conference on Computer Vision and Pattern Recognition*, pages 6047–6056, 2018.
- [18] H. Hajimirsadeghi, W. Yan, A. Vahdat, and G. Mori. Visual recognition by counting instances: A multi-instance cardinality potential kernel. In *Proceedings of the IEEE conference on computer vision and pattern recognition*, pages 2596–2605, 2015.
- [19] M. Han, D. J. Zhang, Y. Wang, R. Yan, L. Yao, X. Chang, and Y. Qiao. Dual-ai: Dual-path actor interaction learning for group activity recognition. In *Proceedings of the IEEE/CVF conference on computer vision and pattern recognition*, pages 2990–2999, 2022.
- [20] K. He, G. Gkioxari, P. Dollár, and R. Girshick. Mask r-cnn. In *Proceedings of the IEEE international conference on computer vision*, pages 2961–2969, 2017.
- [21] M. S. Ibrahim, S. Muralidharan, Z. Deng, A. Vahdat, and G. Mori. A hierarchical deep temporal model for group activity recognition. In *Proceedings of the IEEE conference on computer vision and pattern recognition*, pages 1971–1980, 2016.
- [22] T. Jiang, P. Lu, L. Zhang, N. Ma, R. Han, C. Lyu, Y. Li, and K. Chen. RtmPose: Real-time multi-person pose estimation based on mmPose. *arXiv preprint arXiv:2303.07399*, 2023.
- [23] G. Jocher, A. Chaurasia, and J. Qiu. Yolo by ultralytics, 2023.
- [24] D. Kim, J. Lee, M. Cho, and S. Kwak. Detector-free weakly supervised group activity recognition. In *Proceedings of the IEEE/CVF Conference on Computer Vision and Pattern Recognition*, pages 20083–20093, 2022.
- [25] A. Kirillov, E. Mintun, N. Ravi, H. Mao, C. Rolland, L. Gustafson, T. Xiao, S. Whitehead, A. C. Berg, W.-Y. Lo, et al. Segment anything. In *Proceedings of the IEEE/CVF International Conference on Computer Vision*, pages 4015–4026, 2023.
- [26] T. Lan, Y. Wang, W. Yang, S. N. Robinovitch, and G. Mori. Discriminative latent models for recognizing contextual group activities. *IEEE transactions on pattern analysis and machine intelligence*, 34(8):1549–1562, 2011.

- [27] Y. LeCun, B. Boser, J. Denker, D. Henderson, R. Howard, W. Hubbard, and L. Jackel. Handwritten digit recognition with a back-propagation network. *Advances in neural information processing systems*, 2, 1989.
- [28] A. Li, M. Thotakuri, D. A. Ross, J. Carreira, A. Vostrikov, and A. Zisserman. The ava-kinetics localized human actions video dataset. *arXiv preprint arXiv:2005.00214*, 2020.
- [29] S. Li, Q. Cao, L. Liu, K. Yang, S. Liu, J. Hou, and S. Yi. Groupformer: Group activity recognition with clustered spatial-temporal transformer. In *Proceedings of the IEEE/CVF International Conference on Computer Vision*, pages 13668–13677, 2021.
- [30] Y. Li, L. Chen, R. He, Z. Wang, G. Wu, and L. Wang. Multisports: A multi-person video dataset of spatio-temporally localized sports actions. In *Proceedings of the IEEE/CVF International Conference on Computer Vision*, pages 13536–13545, 2021.
- [31] Y. Li, C.-Y. Wu, H. Fan, K. Mangalam, B. Xiong, J. Malik, and C. Feichtenhofer. Mvitv2: Improved multiscale vision transformers for classification and detection. In *Proceedings of the IEEE/CVF conference on computer vision and pattern recognition*, pages 4804–4814, 2022.
- [32] Z. Li, X. Chang, Y. Li, and J. Su. Skeleton-based group activity recognition via spatial-temporal panoramic graph. In *European Conference on Computer Vision*, pages 252–269. Springer, 2025.
- [33] T.-Y. Lin, M. Maire, S. Belongie, J. Hays, P. Perona, D. Ramanan, P. Dollár, and C. L. Zitnick. Microsoft coco: Common objects in context. In *Computer Vision–ECCV 2014: 13th European Conference, Zurich, Switzerland, September 6–12, 2014, Proceedings, Part V 13*, pages 740–755. Springer, 2014.
- [34] M. Nabi, A. Bue, and V. Murino. Temporal poselets for collective activity detection and recognition. In *Proceedings of the IEEE International Conference on Computer Vision Workshops*, pages 500–507, 2013.
- [35] M. A. Nugroho, S. Woo, S. Lee, J. Park, Y. Wang, D. Kim, and C. Kim. Flow-assisted motion learning network for weakly-supervised group activity recognition. *arXiv preprint arXiv:2405.18012*, 2024.
- [36] D. Pei, D. Huang, L. Kong, and Y. Wang. Key role guided transformer for group activity recognition. *IEEE Transactions on Circuits and Systems for Video Technology*, 33(12):7803–7818, 2023.
- [37] M. Perez, J. Liu, and A. C. Kot. Skeleton-based relational reasoning for group activity analysis. *Pattern Recognition*, 122:108360, 2022.
- [38] R. R. A. Pramono, Y. T. Chen, and W. H. Fang. Empowering relational network by self-attention augmented conditional random fields for group activity recognition. In *European Conference on Computer Vision*, pages 71–90. Springer, 2020.
- [39] T. Shu, D. Xie, B. Rothrock, S. Todorovic, and S. Chun Zhu. Joint inference of groups, events and human roles in aerial videos. In *Proceedings of the IEEE conference on computer vision and pattern recognition*, pages 4576–4584, 2015.
- [40] V. Stanojević and B. Todorović. Boosttrack++: using tracklet information to detect more objects in multiple object tracking. *arXiv preprint arXiv:2408.13003*, 2024.
- [41] W. Su, X. Zhu, C. Tao, L. Lu, B. Li, G. Huang, Y. Qiao, X. Wang, J. Zhou, and J. Dai. Towards all-in-one pre-training via maximizing multi-modal mutual information. In *Proceedings of the IEEE/CVF Conference on Computer Vision and Pattern Recognition*, pages 15888–15899, 2023.
- [42] M. Tancik, P. Srinivasan, B. Mildenhall, S. Fridovich-Keil, N. Raghavan, U. Singhal, R. Ramamoorthi, J. Barron, and R. Ng. Fourier features let networks learn high frequency functions in low dimensional domains. *Advances in neural information processing systems*, 33:7537–7547, 2020.
- [43] H. Thilakarathne, A. Nibali, Z. He, and S. Morgan. Pose is all you need: The pose only group activity recognition system (pogars). *Machine Vision and Applications*, 33(6):95, 2022.
- [44] J. Wu, L. Wang, L. Wang, J. Guo, and G. Wu. Learning actor relation graphs for group activity recognition. In *Proceedings of the IEEE/CVF Conference on computer vision and pattern recognition*, pages 9964–9974, 2019.
- [45] Y. Xu, J. Zhang, Q. Zhang, and D. Tao. Vitpose: Simple vision transformer baselines for human pose estimation. *Advances in neural information processing systems*, 35:38571–38584, 2022.
- [46] R. Yan, L. Xie, J. Tang, X. Shu, and Q. Tian. Hgcin: Hierarchical graph-based cross inference network for group activity recognition. *IEEE transactions on pattern analysis and machine intelligence*, 45(6):6955–6968, 2020.
- [47] R. Yan, L. Xie, J. Tang, X. Shu, and Q. Tian. Social adaptive module for weakly-supervised group activity recognition. In *Computer Vision–ECCV 2020: 16th European Conference, Glasgow, UK, August 23–28, 2020, Proceedings, Part VIII 16*, pages 208–224. Springer, 2020.
- [48] J. Yang, A. Zeng, R. Zhang, and L. Zhang. X-pose: Detecting any keypoints. In *European Conference on Computer Vision*, pages 249–268. Springer, 2025.
- [49] K. Yi, K. Luo, X. Luo, J. Huang, H. Wu, R. Hu, and W. Hao. Ucmtrack: Multi-object tracking with uniform camera motion compensation. In *Proceedings of the AAAI conference on artificial intelligence*, volume 38, pages 6702–6710, 2024.
- [50] H. Yuan, D. Ni, and M. Wang. Spatio-temporal dynamic inference network for group activity recognition. In *Proceedings of the IEEE/CVF International Conference on Computer Vision*, pages 7476–7485, 2021.
- [51] S. Yun, D. Han, S. J. Oh, S. Chun, J. Choe, and Y. Yoo. Cutmix: Regularization strategy to train strong classifiers with localizable features. In *Proceedings of the IEEE/CVF international conference on computer vision*, pages 6023–6032, 2019.
- [52] C. Zach, T. Pock, and H. Bischof. A duality based approach for realtime tv-l 1 optical flow. In *Pattern Recognition: 29th DAGM Symposium, Heidelberg, Germany, September 12–14, 2007. Proceedings 29*, pages 214–223. Springer, 2007.
- [53] H. Zhang, M. Cisse, Y. N. Dauphin, and D. Lopez-Paz. mixup: Beyond empirical risk minimization. *arXiv preprint arXiv:1710.09412*, 2017.

- [54] Z. Zhong, L. Zheng, G. Kang, S. Li, and Y. Yang. Random erasing data augmentation. In *Proceedings of the AAAI conference on artificial intelligence*, volume 34, pages 13001–13008, 2020.
- [55] H. Zhou, A. Kadav, A. Shamsian, S. Geng, F. Lai, L. Zhao, T. Liu, M. Kapadia, and H. P. Graf. Composer: compositional reasoning of group activity in videos with keypoint-only modality. In *European Conference on Computer Vision*, pages 249–266. Springer, 2022.
- [56] Z. Zong, G. Song, and Y. Liu. Detsr with collaborative hybrid assignments training. In *Proceedings of the IEEE/CVF international conference on computer vision*, pages 6748–6758, 2023.

PromptGAR: Flexible Promptive Group Activity Recognition

Supplementary Material

O	Memory	Top1	Mean	ϵ	Top1	Mean
16	40 GB	95.8	96.0	0	95.4	95.6
48	72 GB	96.0	96.3	5	95.6	95.9
56	<i>OOM</i>	-	-	10	95.8	96.0

Table 8. # of Pooled Prompts O . Table 9. Relative Instance Scale ϵ .

Method	Modalities				Head Inputs		Re-train	Top1	Mean
	RGB	Bbox	Kpt	InstID	$\widehat{\mathbf{X}}_{gar}$	$\widehat{\mathbf{F}}_p$			
PromptGAR	✓	✓	✓	✓	✓	✓	×	96.0	96.3
	✓		✓	✓	✓	✓		95.7	95.8
	✓	✓		✓	✓	✓		94.1	94.3
	✓	✓	✓	✓	✓	✓		95.8	96.0
	✓		✓	✓	✓	✓		95.5	95.7
	✓	✓		✓	✓	✓		94.0	94.2
	✓			✓	✓	✓		93.9	94.4
	✓	✓	✓	✓		✓		95.2	95.6
	✓		✓	✓		✓		95.2	95.6
	✓	✓		✓		✓		93.4	94.0

Table 10. Ablation on Head Input Tokens.

1. More on Implementation Details

Data Augmentations. Following MViTv2 in action recognition [31], we apply a comprehensive set of augmentations for group activity recognition (GAR): Random Augment [11], Random Resized Crop, Flip, Random Erasing [54], CutMix [51], and MixUp [53]. In the multi-group activity recognition (Multi-GAR) task, we remove the CutMix and MixUp, because it would be impossible to determine which specific group from the reference frame is being overlaid onto the target frame within the same area prompt.

Volleyball Dataset [21]. Since Volleyball only contains annotations with central 16 frames, we replace the depth-wise prompt pooling with a single MLP layer projecting channels from $T \times 20$ to the number of pooled prompts O .

NBA Dataset [47]. We regenerated annotations due to inaccuracies in SAM [47] and MP-GCN [32], such as background audience false positives, player ID switching, and ID reassignment upon reappearance. We used MOTIP [14] for robust player tracking, optimized for sports data, and RTMPose [22] for accurate skeleton generation, handling occlusions effectively.

2. Additional Ablation Studies

Number of Pooled Prompts. Tab. 8 explores the impact of the number of pooled prompt channels (O) on performance. The prompt encoder’s output has the shape $D \times N \times O$, where D, N, O are the feature dimension, the number of instances, and the pooled prompt channels after

pooling along temporal and prompt type dimensions, respectively. A smaller O value reduces the representativeness and expressiveness of each actor’s key information. As shown in the table, increasing O from 16 to 48 improves top1 accuracy by 0.2%. However, this increase quadratically raises the computational cost and CUDA memory usage of the subsequent recognition decoder module. Specifically, the CUDA memory usage for $O = 48$ is 32 GB higher than for $O = 16$. Further increasing O to 56 would exceed the 80 GB limit of an A100 GPU’s CUDA memory, resulting in an out-of-memory error. Therefore, while a higher O value improves performance, a balance must be struck to avoid excessive computational demands and memory limitations.

Relative Instance Scale. Tab. 9 details the process of determining the optimal relative instance scale, denoted as ϵ . This value serves as a coefficient for the relative instance weights, which are added to the standard attention weights. Due to the inherent sparsity of the relative instance weight matrix $E^{(rel)}$, a small ϵ value would diminish the impact of instance IDs during training. Conversely, an excessively large ϵ would overpower the standard attention weights, hindering the GAR class token’s ability to learn effectively from the prompt tokens. The table reveals that setting ϵ to 10 yields a 0.4% improvement in top-1 accuracy compared to setting it to 0 (effectively disabling relative instance attention) and a 0.2% improvement compared to setting it to 5. Therefore, we selected 10 as the final ϵ value. Notice that these experiments are conducted with a pooled prompt channel count (O) of 16.

Head Inputs Tab. 10 indicates demonstrates the significance of prompt token inputs within the head, even when dealing with multi-modal prompts. We compared performance using a model trained on full prompts, varying the head inputs during testing. Under full modality inputs, using only the GAR class token $\widehat{\mathbf{X}}_{gar}$ as the head input resulted in a minor 0.2% performance drop, while using only the prompt tokens $\widehat{\mathbf{F}}_p$ led to a 0.8% drop. This shows that both inputs are crucial for PromptGAR’s high performance. Even with reduced modality inputs, both $\widehat{\mathbf{X}}_{gar}$ only and $\widehat{\mathbf{F}}_p$ only still yielded reasonable results. Notably, when using only prompt tokens $\widehat{\mathbf{F}}_p$, the performance of full prompt inputs was similar to the one with skeleton-only inputs. This suggests that when RGB features don’t directly influence the final prediction, bounding box information is effectively captured within the skeleton data. In summary, this table showcases the flexibility of head inputs across various modalities and underscores the importance of both the RGB feature representation $\widehat{\mathbf{X}}_{gar}$ and the prompt feature representation $\widehat{\mathbf{F}}_p$ for optimal performance.

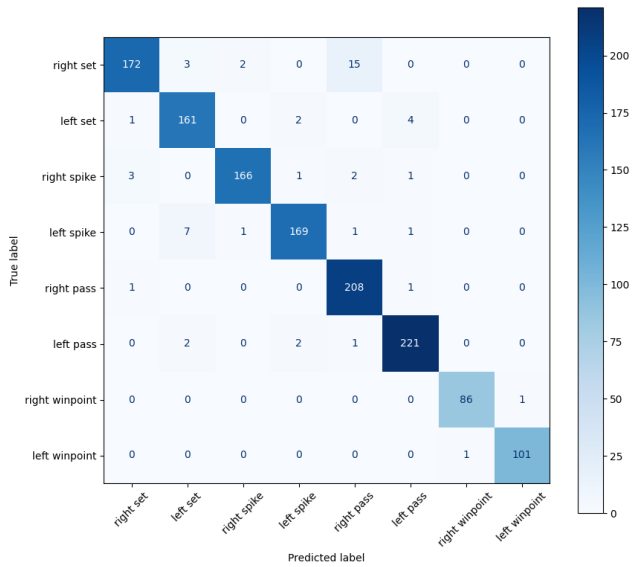


Figure 7. Volleyball Confusion Matrix

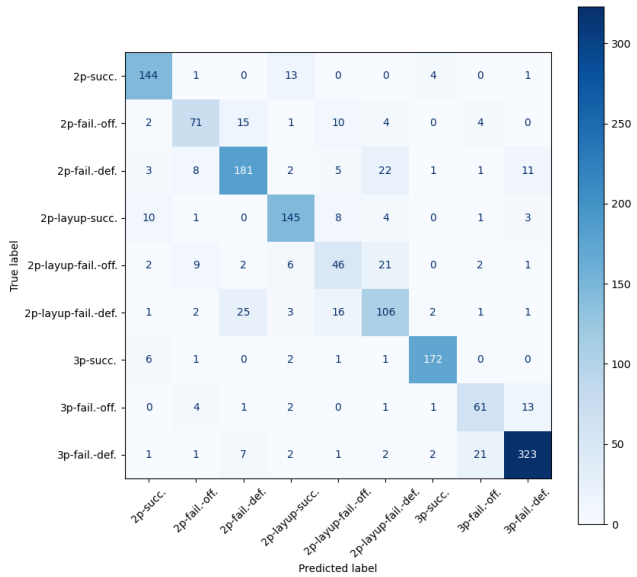


Figure 8. NBA Confusion Matrix

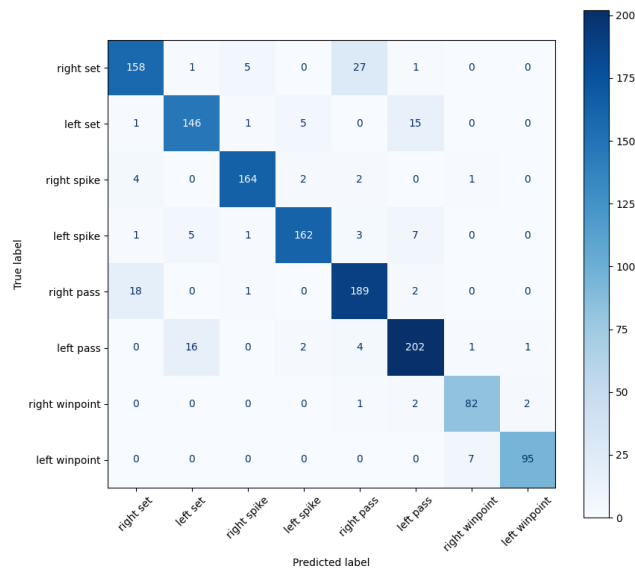


Figure 9. The 2-Mosaic Volleyball Confusion Matrix

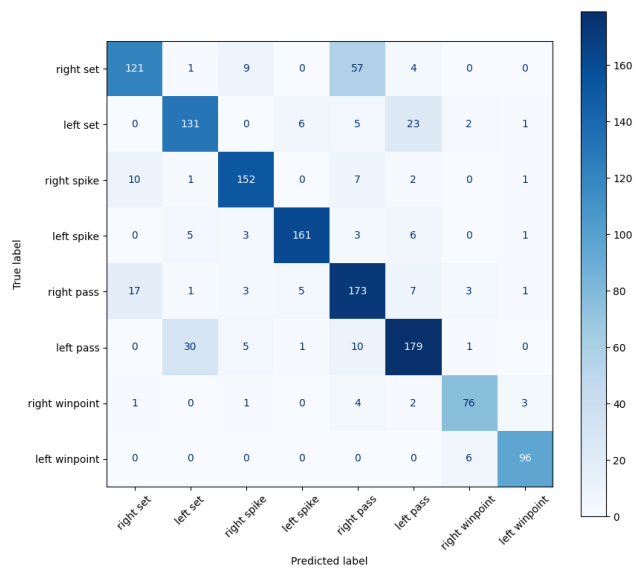


Figure 10. The 4-Mosaic Volleyball Confusion Matrix

3. Analysis

Quantitative Results. Fig. 7 - 10 shows the confusion matrix of Volleyball, NBA, 2-Mosaic Volleyball, and 4-Mosaic Volleyball respectively. (a) For Volleyball, while PromptGAR demonstrates high accuracy on the Volleyball dataset, a common misclassification occurs where ‘right-set’ is mistaken for ‘right-pass’. This error is attributed to the inherent similarity in player actions and positions, echoing findings in previous research [55]. (b) For NBA, errors highlight the challenge of distinguishing between highly similar actions. Specifically, differentiating ‘offensive’ and

‘defensive’ requires nuanced visual analysis of player uniform differences and rebound outcomes. Similarly, distinguishing ‘2p-fail’ from ‘2p-layup-fail’ demands precise attention to shooting position and posture near the rim. (c) In the 2-Mosaic and 4-Mosaic Volleyball datasets, PromptGAR achieves respectable results, despite the significant challenge of reduced actor size and motion blur. This difficulty arises because, while the input image size is doubled (or quadrupled), the model’s input resolution remains fixed at 224×224 . Given that only area prompts are provided, without any additional enhancement information, the model struggles to distinguish between ‘pass’ and ‘set’ activities.